

EXPERIMENTAL INVESTIGATION OF SOLAR COMPOUND PARABOLIC COLLECTOR USING Al_2O_3/H_2O NANOFLUID IN A SUBTROPICAL CLIMATE

by

**Faria AKHTAR^a, Muzaffar ALI^{a*}, Nadeem Ahmed SHEIKH^b,
and Muhammad SHEHRYAR^c**

^a Energy Engineering Department,
University of Engineering and Technology Taxila, Taxila, Pakistan

^b Faculty of Engineering and Technology,
International Islamic University Islamabad, Islamabad, Pakistan

^c Mechanical Engineering Department,
University of Engineering and Technology Taxila, Taxila, Pakistan

Original scientific paper
<https://doi.org/10.2298/TSCI191207201A>

Different solar concentrator technologies are used for low medium range temperature applications. In this paper, a non-tracking compound parabolic collector with a nanofluid is experimentally analyzed under real climate conditions of a typical sub-tropical climate Taxila, Pakistan. The collector used for the experimentation has concentration ratio of 4.17, collector area of 0.828 m² and half acceptance angle of 24°. The heat transfer fluid used for the study is water based nanofluid with particles of Al₂O₃. The investigation is carried out at three different volumetric concentrations (0.025%, 0.05%, and 0.075%) of nanofluids at flowrates of 0.01 kg/s, 0.02 kg/s, 0.05 kg/s, and 0.07 kg/s are compared with base fluid (water). Comparison of system thermal efficiency, solar heat gain, and temperature difference is presented for different selected days in real climate conditions during months of March to May. It is observed that performance of the compound parabolic collector is improved by 8%, 11%, 14%, and 19%, respectively, at considered flow rates compared to water.

Key words: *compound parabolic collector; nanofluid; thermal analysis, solar thermal systems*

Introduction

Solar energy is the most common and abundant form of renewable energy available in most parts of the world with an approximate potential of around 3.0 million MW [1]. The building sector has significant share in the total world energy demand. For instance, in developed countries like the USA, about 50% energy is used by building sector, which is mainly utilized for heating, cooling, and other applications. In Pakistan, the annual consumption of energy in building sector is around 30% which indicates an expansion in energy use in the building sector for developing countries [2]. Apart of the building sector, several industrial processes are also being executed in low to medium range temperature limits. For this intermediate limit, the temperatures lie from about 60-200 °C which is a typical operating zone which can be covered by various solar thermal collectors. Various daily domestic and commercial

* Corresponding author, e-mail: muzaffar.ali@uettaxila.edu.pk

involve low and moderate quality heat applications such as textile, paints, and food industries as well as space heating, ventilation, and air conditioning (HVAC) applications [3, 4]. Flat and evacuated tube collectors are considered for low range temperature applications, while solar concentrators are deemed as medium to high range temperatures solar thermal collectors. Amongst the concentrating solar collectors, parabolic trough collector is the most proven industry scale solar heat generation technology [5]. The key solar system for the medium range temperatures is the compound parabolic collector (CPC) for solar thermal driven applications in different sectors.

The HVAC systems are the main source of energy demand in building sector, especially in summer due to gradually increase in space heating, cooling, and ventilation requirements [6]. In this situation, the use of solar energy via solar thermal systems can play a vital role to overcome the energy crisis and to reduce the dependency upon traditional fossil fuels [7]. In thermal market, the low range temperature solar thermal collectors such as flat plate, evacuated tube and small-scale CPC cover significant share of building sector for heating [8, 9]. A study investigated a non-tracking CPC with evacuated tube receiver resulting an optical performance 65% and thermal effectiveness as 50% [10]. The tracking system with any solar thermal collector can result to improve the overall efficiency of the system but it comes with actuation system and is relatively expensive. A comprehensive study proved that the solar collector with tracking has performed 15% better than stationary collector [11]. In another study, two new compound parabolic trough and dish solar collectors were analyzed. It was observed that efficiency is improved about 10% and 20% for linear and convoluted models, respectively [12].

A solar water heating system (SWHS) was also assessed and compared with traditional heating fuels for climatic conditions of Greece. The ratio of benefit cost for SWHS usage in different sectors like in household, hospital and restaurant was 5.76, 2.74, and 1.31, respectively, [13]. In addition, an experimental study presented the optical and thermal performance of CPC along with evacuated tube receiver. This study consisted of two parts: geometry design of CPC and the thermal analysis of solar collectors. It also explained the optical efficiencies of CPC at different solar angles along its losses [14]. In another study, different design was proposed to overcome the limitations of CPC related to height, width and low concentration. The geometry of this study was design with low focus point of parabola and vertical position of receiver for better optical performance. The set point of the reflector was at a height of 0.46 times compared to its width, *i.e.* $H = 0.46D$ [15].

Performance of solar thermal collector is significantly influenced by heat transfer characteristics of the working fluid. Therefore, nanofluids compared to conventional fluids can play a vital role to improve the thermal enhancement of such system. In this regard, a study suggested that the enhancement of heat transfer by suspended nanosized metallic and non-metallic materials [16] can be significant. The effect of nanoparticles size and their concentration on thermal enhancement and conductivity was also analyzed as a key performance parameter [17]. Moreover, a comprehensive study investigated the thermophysical properties of nanofluids for enhanced convective heat transfer [18]. Similarly, aqueous based carbon nanofluid was also analyzed [19] along their effects on mass fraction, temperature, pH and different surfactants. Another study emphasized on rod-shaped TiO_2 nanofluid with deionized water. The thermal enhancement was achieved by 33% using 5% volumetric nanofluid concentration in deionized water [20].

Different types of nanosized metal and metal oxide particles have been prepared and tested with various base fluids in terms of their key characteristics. For example, the morphology for different nanoparticles were presented [21]. The results of increasing heat transfer coefficient using different volumetric concentration of aluminum oxide nanofluid were also examined

[22]. The effect of temperature and viscosity for iron based nanofluids on distinct concentration ratio was analyzed [23]. Another experimental study evaluated a solar thermal system with TiO_2 -water nanofluid having 0.2% volumetric concentration. It was observed that the nanofluid improved the heat transfer coefficient 6-11% compared to water [24]. Furthermore, Cu-water and TiO_2 -water nanofluids had enhanced free convection when used in a square cavity with a heat source on the bottom wall [25]. Similarly, enhancement of natural-convection heat transfer in a U-shaped cavity filled with Al_2O_3 -water nanofluid was presented [26]. In a parabolic trough system, the maximum efficiencies achieved with Al_2O_3 and Fe_2O_3 nanofluids at 2 Lpm were 13% and 11% higher, respectively compared to water [27].

Keeping in view the relevant literature, it can be observed that many studies are focused on geometric aspects of solar collectors and utilization of nanofluids in various heat exchangers, especially in parabolic trough collector. However, effects of efficiency enhancement of non-tracking CPC with metallic oxide based nanofluid like Al_2O_3 are rarely analyzed. Therefore, in the present work, extensive experiments are conducted and reported having two aspects which are novel:

- For subtropical climate conditions, a detailed experimental analysis under transient climate conditions is presented for CPC systems which is rarely conducted. In addition, Al_2O_3 -water nanofluid with wide range of different volumetric concentrations is used in this system for comparative experimental analysis of CPC with water under same operating and climate conditions.
- The developed system presented here utilized totally local available materials and facilities for fabrication. The thermal performance of such a CPC system under different ambient and operating conditions add significant value through these results, especially for regional deployments.

The system designs

In the current study, the solar thermal system consists of CPC, storage tank and pump for circulation of water/nanofluid. The main purpose of storage tank is to provide a constant output. The effectiveness of the thermal system mainly depends on different parameters of CPC including its geometry, acceptance angle, orientation and solar irradiance on a specific day. The schematic diagram for the proposed CPC solar system is shown in fig. 1.

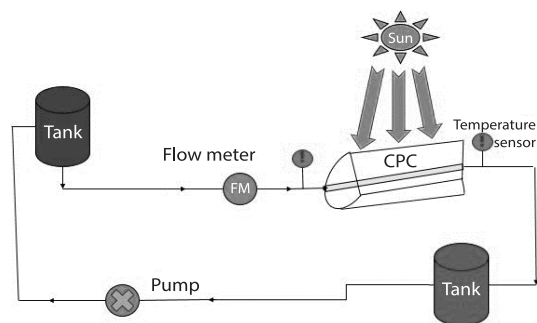


Figure 1. The system schematic diagram

Design of CPC system

The design of the CPC geometry is based on well-established set of equations to determine all geometric parameters. A key aspect in geometry design is truncation of trough which is applied to reduce the cost of collector sheet material without disturbing the performance of CPC. Therefore, in this study, the parabolic sides of the CPC are truncated by 20% to lower the height and cost of CPC. The collector aperture width and height and other design specifications are shown in fig. 2. The total width of collector, $2a$, is reduced to 0.4455 m , $2a_T$, after truncation. The half acceptance angle, θ_c , for the system is estimated to be around 24° . The specifications of CPC are mentioned in tab. 1.

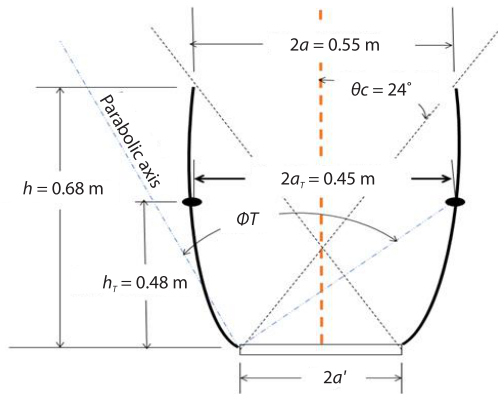


Figure 2. The cross-sectional view of CPC

Table 1. Solar system design specifications

Parameter	Value
Collector area [m ²]	0.828
Aperture length [m]	1.858
Aperture width [m]	0.4456
Half acceptance angle [°]	24
Concentration ratio	4.17
Receiver tube length [m]	1.858
Absorber outer diameter [mm]	34
Glass outer diameter [mm]	60
Thickness [mm]	2.5

The slope of collector depends upon solar declination and country latitude:

$$\delta = 23.5 \sin \left[\frac{360}{365} (N + 284) \right] \quad (1)$$

The tilt angle, β , calculated as:

$$\beta = \varphi + \delta \quad \text{during winter}$$

$$\beta = \varphi - \delta \quad \text{during summer}$$

Optical efficiency is a vital performance parameter for CPC. The most comprehensive equation for optical efficiency is [28]:

$$\mu_0 = \rho\tau\alpha\gamma \quad (2)$$

where γ is the accuracy intercept for construction whose value lies in the range of 0.9-1.0, the other parameters are collector wall reflectivity, sheet transmittance and absorptivity of the receiver. The solar thermal systems are judged by its thermal efficiency which is the ratio of solar heat energy gained to the product of collector aperture area and available global solar radiations. The useful solar gain is obtained [28]:

$$Q_u = A_a F_r \left[I_G - \left\{ \frac{U_L}{C} (T_i - T_a) \right\} \right] \quad (3)$$

$$F_r = \frac{m'c_p}{A_r U_L} \left[1 - \exp \left(- \frac{A_r U_L F'}{m'c_p} \right) \right] \quad (4)$$

Concentration ratio of solar thermal collector is determined:

$$C = \frac{A_a}{A_r} \quad (5)$$

The thermal efficiency of CPC was calculated:

$$\eta = \frac{Q_u}{Q_s} \times 100 \quad (6)$$

The useful solar collector gain can also be calculated:

$$Q_u = m'c_p (T_i - T_o) \quad (7)$$

Whereas the energy supplied, Q_s , is found:

$$Q_s = A_a I_G \quad (8)$$

The incident angle modifier (IAM) is calculated in terms of thermal efficiency, collector heat removal factor and optical efficiency [29]:

$$IAM = \frac{\eta T_i}{F_r \mu_0} \quad (9)$$

Whereas the density and specific heat of the nanofluid are determined [27]:

$$\rho_{nf} = (1 - \varphi) \rho_{bf} + \varphi \rho_{np} \quad (10)$$

$$c_{pnf} = (1 - \varphi) c_{pbf} + \varphi c_{pnp} \quad (11)$$

The experimental set-up and measurement procedure

The experimental set-up is installed at Energy Department of University of Engineering and Technology, Taxila, Pakistan. The location and orientation of CPC are decided by sun path finder apparatus. The most feasible orientation install the CPC is horizontal *E-W*-axis facing south because in this direction the availability of sun light throughout the day is higher than the *N-S*-direction. The concentration ratio for the collector used for the study is 4.17, with collector area of 0.8 m². The evacuated tube receiver has the area as 0.2 m² with length of 1.85 m. The collector temperatures are measured by fiber optic temperature sensor. The experimental set-up of the CPC is shown in fig. 3.

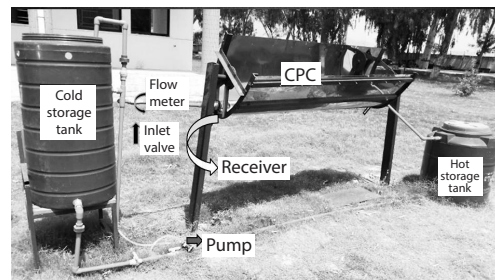


Figure 3. Experimental set-up of solar CPC system

The experimental set-up is made as a close loop to investigate thermal efficiency of CPC system. First, the leakage at every port is checked and appropriate flow rates were ensured. The cold water enters from pump to the CPC which heats up water. Hot water from collector enters the storage tank for steady output. The water from the outside of tank goes towards source side. The *K*-type sensors are installed at the inlet and outlet valves to monitor the temperatures through a data acquisition system. The flow rate for water is measured by flow meter which is installed at the inlet port. Hourly solar radiations are measured by pyranometer. The ambient temperature is recorded by fiber optic temperature sensor. During experimentation different flow rates (0.01-0.07 kg/s) and volumetric concentrations of nanofluids are varied. Three concentrations of metallic oxide nanofluids are 0.025%, 0.05%, and 0.075%.

The experimental readings are measured after every 15 minutes. Moreover, for accurate data collection the readings were repeated at least for two-three days at same flow. After every experiment, nanofluid needs to be re-blended before the next day experimentation for ensuring mixing and to avoid the stability issues. The experimentations are carried out on around 35 selected days between the months of March to May 2019 to account for the variations in solar intensity and natural variations. The monitoring time for experimentation is 9:00 a. m. to 3:00 p. m. on hourly basis on each of the selected day.

Measurement equipment and error analysis

The operating collector temperatures are measured by using thermocouples (*K*-type) having susceptibility of $\pm 0.1^\circ\text{C}$. Weather data including wind velocity and solar radiations are measured through anemometer and pyranometer (model TBS-2) with sensitivity 280-3000 ns and 1-3 W/m^2 , respectively. The heat transfer fluid (HTF) flow rate is measured through a flow sensor (model: OKY3430-0) with flow range 1-30 Lpm as given in tab. 2. The uncertainty in the thermal efficiency of system is calculated by root square method [27].

If $\alpha = f(b_1, b_2, b_3, b_4, b_5, b_6, b_7\dots)$

$$C_a = \sqrt{\left(\frac{\delta\alpha}{\delta b_1} C b_1\right)^2 + \left(\frac{\delta\alpha}{\delta b_2} C b_2\right)^2 + \left(\frac{\delta\alpha}{\delta b_3} C b_3\right)^2 + \left(\frac{\delta\alpha}{\delta b_4} C b_4\right)^2 \dots} \quad (12)$$

The overall error for the thermal performance is calculated as about 3.5%.

Table 2. Uncertainty of apparatus used in data measurement

Parameters	Apparatus	Uncertainty level
Collector temperature	<i>K</i> -type thermocouple	$\pm 0.1^\circ\text{C}$
HTF Flow rate	Flow sensor	+2%
Solar radiation	Pyranometer	1-3 W/m^2

Table 3. Properties of nanoparticle Al_2O_3 [27]

Parameter	Value
Average diameter [nm]	20
Morphology	Spherical
Particle color	White
Particle specific heat [$\text{Jkg}^{-1}\text{K}^{-1}$]	880
Particle density [kgm^{-3}]	3890

Preparation of nanofluids

In this study, nanosized metallic oxide particles are used for thermal enhancement of solar collector system. Highly pure nanoparticles are bought from US Research Nanomaterials, Inc. The specific properties of nanofluids are given in tab. 3.

The present method which is used to prepare nanofluids is two steps preparation process.

In the first step, the selective concentration of grained nanoparticles is mixed with distilled water. Then magnetic stirrer is used at 340 rpm frequency to stirrer the fluid. Stirring at such high frequency leads to breakage of grains of nanoparticles to mix them into base fluid. While in the second step, covalent bonds between the particles are broken down with the aid of ultrasonic vibrator. The sonication of nanofluid decreases the space of mixture and homogenize them. The sonication for these nanofluids has been done for 5-6 hours so that the mixture remains stabilize for longer duration. The maximum limit of magnetic stirrer to provide frequency is 1150 rpm while the sonication bath has the capacity up to 5.75 L.

The thermophysical properties of water and nanofluid with selected volumetric concentration ratio of nanofluid (0.075%) are given in tab. 4.

Table 4. Thermo-physical properties of the nanofluid [28]

Type of fluid	ρ [kgm^{-3}]	c_p [$\text{Jkg}^{-1}\text{K}^{-1}$]	μ [$\text{kgm}^{-1}\text{s}^{-1}$]	K [$\text{Wm}^{-1}\text{K}^{-1}$]
Water	1000	4190	0.00063	0.6301
Al_2O_3 -water	1212.9	3941	0.00052	0.7718

Limitations of nanofluids

Even though nanofluids enhance the heat transfer characteristics but there are a few limitations to use them, for example:

- Expensive to prepare nanoparticles and production of nanofluids.
- Nanofluids require high flow rates compare to water due to higher densities.
- Sometimes, when the working states of the system are natural-convection and presented to high temperature, the nanoparticles could agglomerate and demonstrate stability issues.
- Nanoparticles can cause corrosion and erosion the metallic parts of the system and block the flow of fluid.
- Nanoparticles are toxic for human health. It may cause etching and allergy if proper precautions are not followed.

Results and discussion

The present work basically is focused on an experimental analysis of thermal enhancement of a metallic oxide nanofluid Al_2O_3 compared to water. The analysis is presented in terms of temperature difference achieved, heat gain, and thermal efficiency of the system under a sub-tropical climate, Taxila, Pakistan. Figure 4 shows variation of climate conditions of the selected location. The overall range of ambient temperature (T) changes from 18.5-38°C, while the wind velocity (WV) varies from 1.9-4.8 m/s. The daily variation of temperature for each considered month is also highlighted. Moreover, the measured solar incident radiations vary throughout the day having maximum value of around 1200 W/m^2 around afternoon as shown in fig. 5. The values are averaged of each hour resulting during all selected days from March to May, 2019.

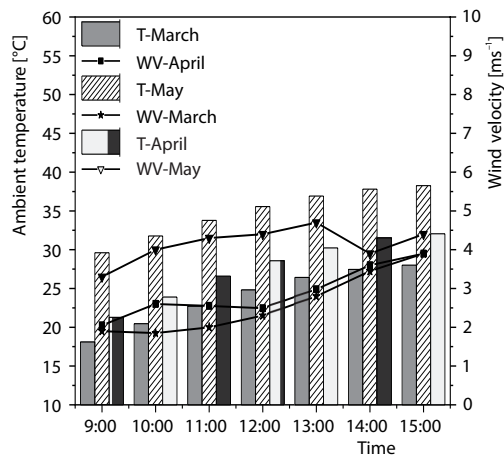


Figure 4. Variation of climate conditions

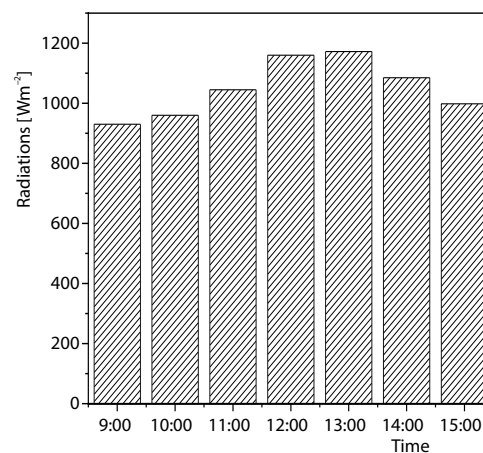


Figure 5. Daily variation of solar radiations

Variation of temperature gain and system thermal efficiency

The system thermal performance is significantly influenced by the temperature difference attained by the CPC system. Variation of temperature difference at four different flow rates is indicated in figs. 6(a)-6(d). For water, temperature difference is increased from 1.7 °C to 7 °C for higher to lowest flow rate *i.e.* 0.01 kg/s. While under same climate conditions, the achieved temperature change is observed by nanofluids around 2.7-10 °C. The maximum temperature gain is resulted with highest concentration of nanoparticles *i.e.* 0.075%. The maximum tem-

peratures are achieved when the solar radiation is at its peak during the day. Overall, nanofluid resulted with higher temperature gradient compared to water under all circumstances.

Similarly, it can be further observed that the efficiency of water as HTF varies from about 12-45% under all considered situations. Whereas the resultant efficiency by using nanofluids varies from 20-76% at different selected mass-flow rates and concentrations of nanoparticles. The increase in efficiency is noted as 8%, 14%, and 19% at three flow rates as 0.01 kg/s, 0.05 kg/s, and 0.07 kg/s, respectively. The maximum values are achieved with the highest nanoparticle concentration when the solar radiations are at its peak.

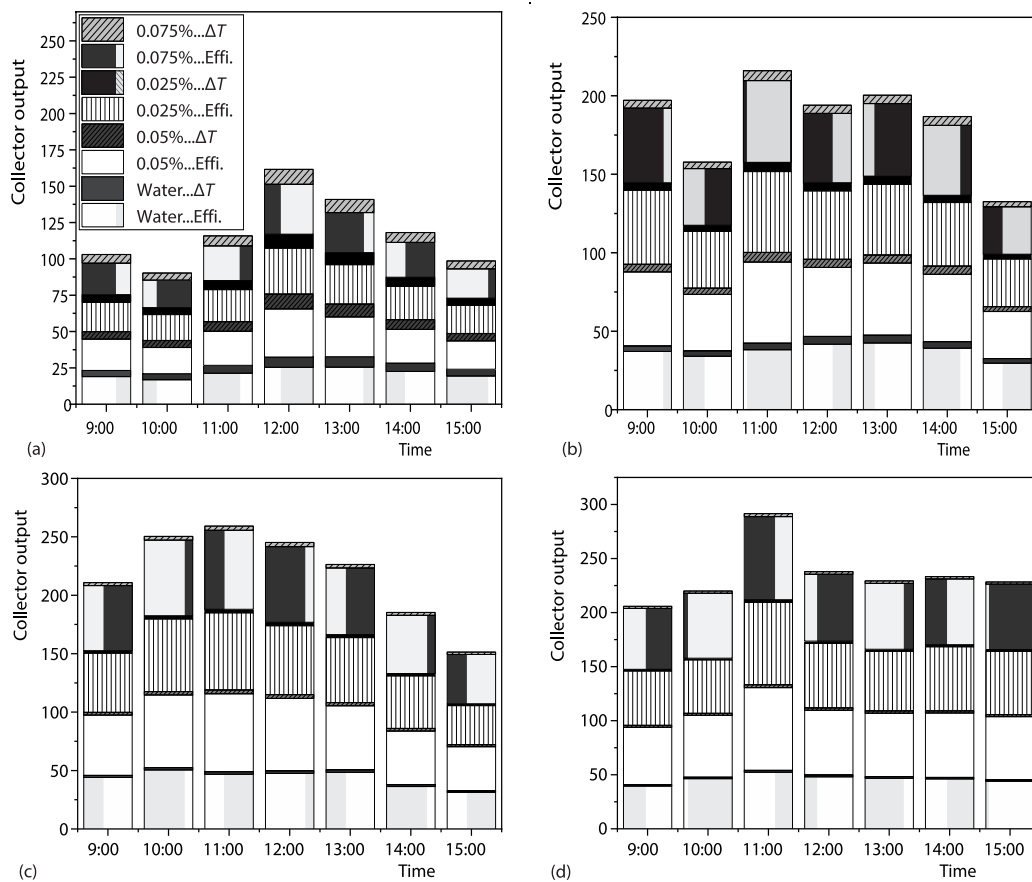


Figure 6. Variation in temperature difference and efficiency with volumetric concentrations at different flow rates; (a) 0.01 kg/s, (b) 0.02 kg/s, (c) 0.05 kg/s, and (d) 0.07 kg/s

Variation of solar heat gain

The solar gain varies with temperature difference and specific heat capacity of fluids at different volumetric concentrations and flow rates. The variation of water and three concentrations of nanofluid are shown in fig. 7. The nanofluids resulted with about 43% enhanced heat gain compared water. The solar heat gain changed from 250-490 W at low flow rate 0.01 kg/s to highest flow as 0.07 kg/s, respectively. At high flow rate the solar gain and efficiency are high but the temperature difference is minimum compare to remaining flowrates. The overall trend

is decided by the dominant increasing or decreasing factor. In overall, the maximum solar heat gain is achieved with the highest concentration and flow rate *i.e.* 690 W.

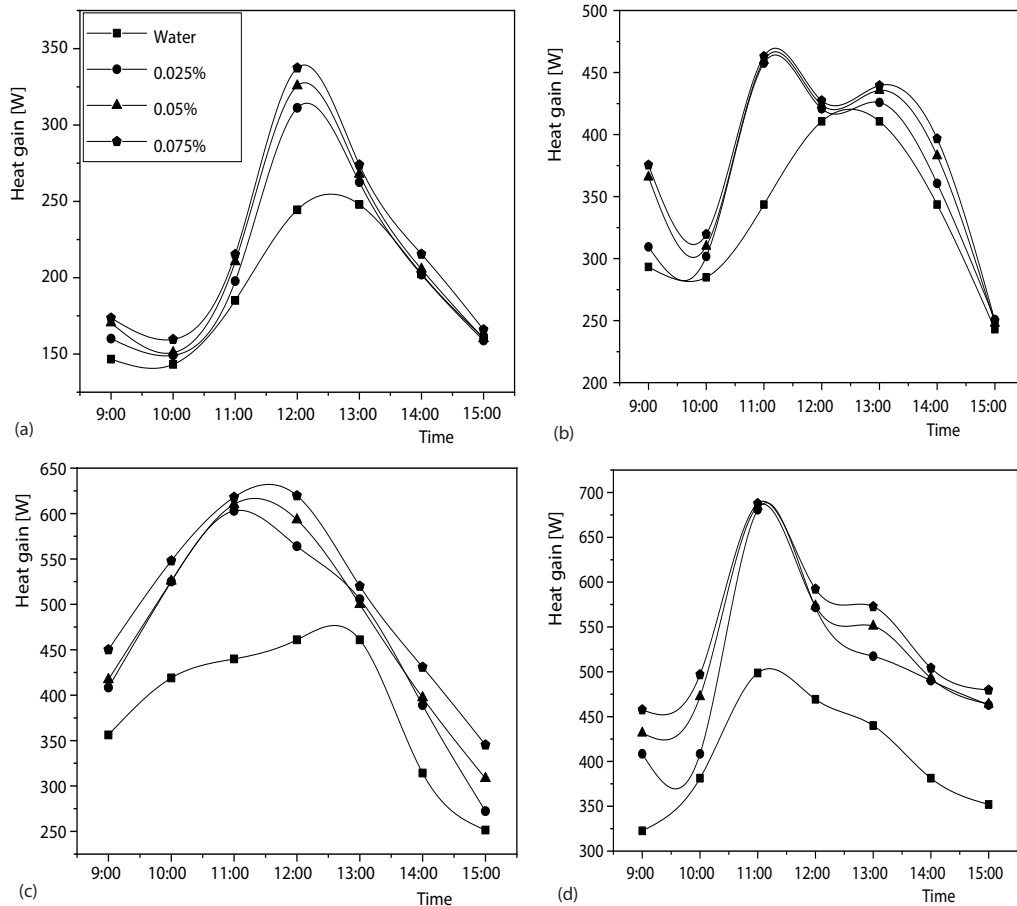


Figure 7. Variation in solar heat gain with volumetric concentrations at different flow rates; (a) 0.01 kg/s, (b) 0.02 kg/s, (c) 0.05 kg/s, and (d) 0.07 kg/s

Figure 8 represents the incidence angle modifier variation with respect to the incidence angle. As the angle of incidence increases, the incidence angle modifier decreases which reduce the coming incident solar radiation. In the current study, the experimentation is performed under wide range of solar radiations of a subtropical climate, Taxila, Pakistan. However, in view of data shown in fig. 9 in which the resulted temperature difference at different flow rates is presented with respect to solar index in W/m^2 . These various solar fluxes indicate different regions. Thus, any interested researcher can mark the average solar index of its region and can easily find out the temperature gain at different flowrate it can achieve through such a system. Thus, the results for other regions are also presented in terms of certain solar radiations which could be more for other climates having a similar range. It can be observed that solar radiations are seemed to be directly proportional to the temperature difference while the flow rate variations have inverse relation. The maximum temperature difference is attained at low flowrate of 0.01 kg/s and at maximum solar radiations.

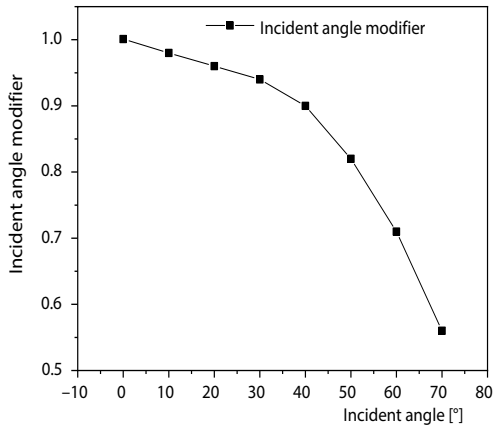


Figure 8. Variation of IAM

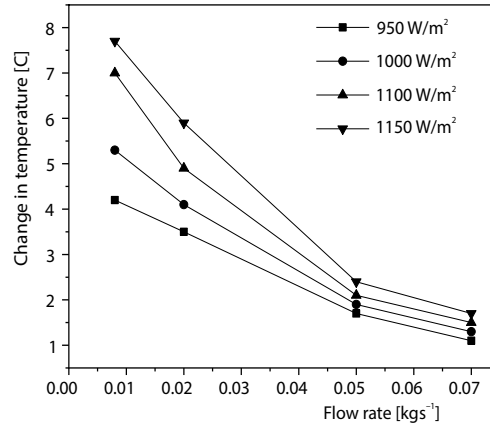


Figure 9. Temperature gain at different solar fluxes and flow rates

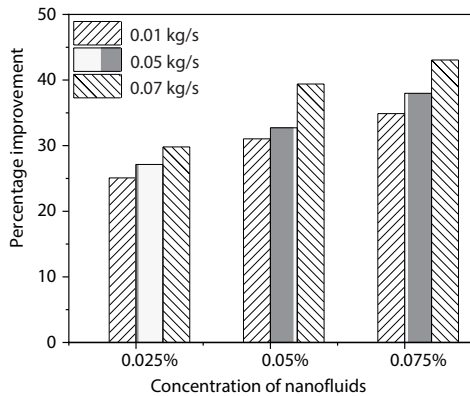


Figure 10. Overall improvement of different volumetric concentrations of the nanofluid

Finally, the overall performance improvement of a CPC system through a Al_2O_3 -water nanofluid is shown in fig. 10. It presents average values of all data sets during whole range of experimentation. It can be analyzed that the maximum increase in the system performance is 43% at the maximum flow rate and concentration of the nanoparticles. It is to be noted that as the current system design and operating conditions are unique in terms of CPC geometric parameters and climate conditions. Therefore, qualitative comparison is included as shown fig. 11. The results of water as working fluid through CPC are compared in terms of collector outlet temperature, and thermal efficiency of flowing water in the absorber-

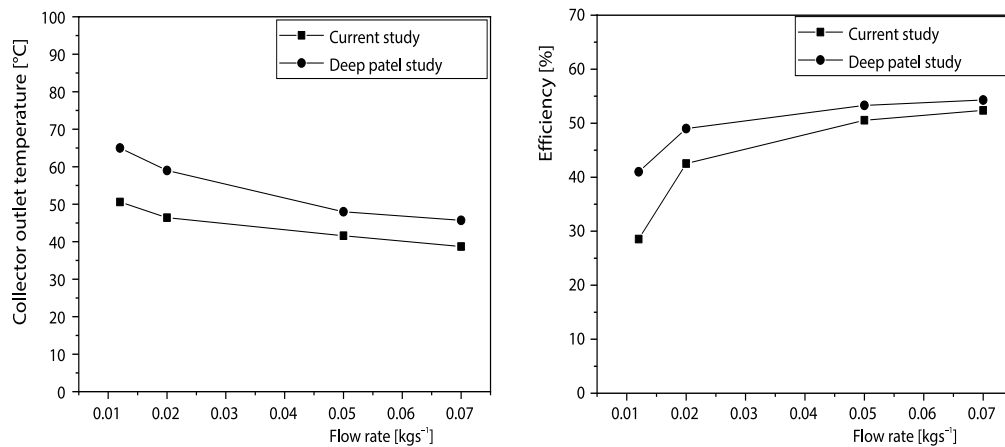


Figure 11. Comparison with published experimental work [30]

er tube of collector with published Deep *et al.* experimental work [30]. It can be observed that trends of effect of mass-flow rate on temperature gain and thermal efficiency are almost similar. Thus, the outcomes of the current work are well comparable with other published results.

Conclusion

In the current work, an experimental analysis of a CPC system using Al_2O_3 metallic oxide based nanofluids as HTF is performed under wide range of real conditions of a sub-tropical climate Taxila, Pakistan. The analysis is performed with different operating conditions in terms of mass-flow rate, concentration of nanoparticles *i.e.* 0.025%, 0.05%, and 0.075%. The maximum temperature difference achieved by Al_2O_3 is 10.75°C at the lowest flow rate. The best system performance is resulted with maximum concentration of nanoparticle *i.e.* 0.075 % when the solar radiation is at its peak. The analysis is conducted parametrically for different ambient temperatures from $30\text{--}37^\circ\text{C}$. The detailed experimental analysis of CPC revealed that HTF heat gain was 340 W and 690 W at low to high working temperatures, respectively. The utilization of nanofluids improves the HTF heat gain by 18.58% for the low working temperatures and up to 21.22% in the high working temperatures. The mean HTF heat gain enhancement is 19.9%. The thermal collector efficiency was 34% and 76% at low to higher flowrate, respectively. The collector efficiency enhancement is found from 8% up to 19%, while the mean thermal efficiency improvement is 13.5%. The mean uncertainty of the system experimental data for the thermal efficiency for all concentrations analyzed as $\pm 3.5\%$, while the increment of temperature was $\pm 0.1^\circ\text{C}$. In addition, the nanofluid resulted an average of 43% enhanced system performance compared to water. Thus, the aluminum oxide based nanofluid is more suitable to enhance the thermal output of a CPC system.

Acknowledgment

Authors are grateful to Higher Education Commission of Pakistan (HEC) for provided funding for this research work through NRP-10483 project.

Nomenclature

a	– aperture width, [m]
a_T	– truncated width, [m]
A_a	– aperture area, [m^2]
A_r	– receiver area, [m^2]
C	– concentration ratio
c_p	– specific heat capacity, [$\text{Jkg}^{-1}\text{K}^{-1}$]
F_r	– collector heat removal factor
F'	– collector efficiency factor
h_T	– truncated height, [m]
I_G	– global radiations, [Wm^{-2}]
N	– No. of days
Q_u	– solar heat gain, [W]
ΔT	– temperature difference, [$^\circ\text{C}$]
T_a	– ambient temperature, [$^\circ\text{C}$]
T_i	– inlet temperature, [$^\circ\text{C}$]
T_o	– outlet temperature, [$^\circ\text{C}$]
U_L	– heat loss coefficient, [$\text{Wm}^{-2}\text{K}^{-1}$]

Greek Letters

α	– absorptivity
β	– slope, [$^\circ$]
γ	– intercept factor
δ	– declination, [$^\circ$]
η	– thermal Efficiency, [%]
θ_c	– acceptance angle, [$^\circ$]
μ_0	– optical efficiency, [%]
ρ	– density, [kgm^{-3}]
τ	– transmittance
ΦT	– truncated angle ($= 80^\circ$)
φ	– latitude [$^\circ$]

Subscripts

bf	– base fluid
nf	– nanofluid
np	– nanoparticle

References

- [1] Ghafoor, A., *et al.*, Current Status and Overview of Renewable Energy Potential in Pakistan for Continuous Energy Sustainability, *Renewable and Sustainable Energy Reviews*, 60 (2016), July, pp. 1332-1342

- [2] Ali, B., et al., *Pakistan Energy Yearbook*, Hydrocarbon Development Institute of Pakistan, Islamabad, Pakistan, 2014
- [3] Kim, Y. S., et al., Efficient Stationary Solar Thermal Collector Systems Operating at a Medium-Temperature Range, *Applied Energy*, 111 (2013), Nov., pp. 1071-1079
- [4] Bellos, E., Tzivanidis, C., A Review of Concentrating Solar Thermal Collectors with and Without Nanofluids, *Journal of Thermal Analysis and Calorimetry*, 135 (2019), Mar., pp. 763-786
- [5] Hachicha, A. A., et al., Heat Transfer Analysis and Numerical Simulation of a Parabolic trough Solar Collector, *Applied Energy*, 111 (2013), Nov., pp. 581-592
- [6] ***, Energy Statistics: Electrical Information 2018, <http://www.iea.org>
- [7] Gunerhan, H., Hepbasli, A., Exergetic Modelling and Performance Evaluation of Solar Water Heating Systems for Building Applications, *Energy and Buildings*, 39 (2007), 5, pp. 509-516
- [8] Li, Q., et al., Design and Analysis of a Medium-Temperature, Concentrated Solar Thermal Collector for Air-Conditioning Applications, *Applied Energy*, 190 (2017), Mar., pp. 1159-1173
- [9] Ayompe, L. M., et al., Validated TRNSYS Model for Forced Circulation Solar Water Heating Systems with Flat Plate and Heat Pipe Evacuated Tube Collectors, *Applied Thermal Engineering*, 31 (2011), 8-9, pp. 1536-1542
- [10] Snail, K. A., et al., A Stationary Evacuated Collector With Integrated Concentrator, *Solar Energy*, 33 (1984), 5, pp. 441-449
- [11] Kim, Y., et al., An Evaluation on Thermal Performance of CPC Solar Collector, *International Communications in Heat and Mass Transfer*, 35 (2008), 4, pp. 446-457
- [12] Sadaghiyani, K. O., et al., Two New Designs of Parabolic Solar Collectors, *Thermal Science*, 18 (2014), Suppl. 2, pp. S323-S334
- [13] Diakoulaki, D., et al., Cost Benefit Analysis for Solar Water Heating Systems, *Energy Conversion and Management*, 42 (2001), 14, pp. 1727-1739
- [14] Bellos, E., et al., Design, Simulation and Optimization of a Compound Parabolic Collector, *Sustainable Energy Technologies and Assessments*, 16 (2016), Aug., pp. 53-63
- [15] Kuo, C.-W., et al., The Design and Optical Analysis of Compound Parabolic Collector, *Procedia Engineering*, 79 (2014), pp. 258-262
- [16] Freegah, B., et al., Computational Fluid Dynamics Based Analysis of a Closed Thermo-Siphon Hot Water Solar System, *Proceedings*, 26th International Congress of Condition Monitoring and Diagnostic Engineering Management, Helsinki, Finland, 2013, pp. 11-13
- [17] Selvakumar, P., Somasundaram, D. P., Effect of Inclination Angle on Temperature Characteristics of Water in-Glass Evacuated Tubes of Domestic Solar Water Heater, *International Journal of Engineering and Innovative Technology*, 1 (2012), 4, pp. 78-81
- [18] Kakac, S., Pramuanjaroenkij, A., Review of Convective Heat Transfer Enhancement With Nanofluids, *International Journal of Heat and Mass Transfer*, 52 (2009), 13-14, pp. 3187-3196
- [19] Amrollahi, A., et al., Conduction Heat Transfer Characteristics and Dispersion Behaviour of Carbon Nanofluids as a Function of Different Parameters, *Journal of Experimental Nanoscience*, 4 (2009), 4, pp. 347-363
- [20] Murshed, S. M. S., et al., Enhanced Thermal Conductivity of TiO₂-Water Based Nanofluids, *International Journal of Thermal Sciences*, 44 (2005), 4, pp. 367-373
- [21] Park, E. J., Park, H. W., Synthesis and Optimization of Metallic Nanofluids Using Electrical Explosion of Wires in Liquids, *Proceedings*, School of Mechanical and Advanced Materials Engineering, Ulsan National Institute of Science and Technology, Ulsan, South Korea, 2011, Vol. 2, pp. 535-538
- [22] Labib, M. N., et al., Numerical Investigation on Effect of Base Fluids and Hybrid Nanofluid in Forced Convective Heat Transfer, *International Journal of Thermal Sciences*, 71 (2013), Sept., pp. 163-171
- [23] Bahrami, M., et al., An Experimental Study on Rheological Behavior of Hybrid Nanofluids Made of Iron and Copper Oxide in a Binary Mixture of Water and Ethylene Glycol, *Experimental Thermal and Fluid Sciences*, 79 (2016), Dec., pp. 231-237
- [24] Duangthongsuk, W., Wongwises, S., Heat Transfer Enhancement and Pressure Drop Characteristics of TiO₂-Water Nanofluid in a Double-Tube Counter Flow Heat Exchanger, *International Journal of Heat and Mass Transfer*, 52 (2009), 7-8, pp. 2059-2067
- [25] Mostafa, M., et al., Free Convection of a Nanofluid in a Square Cavity with a Heat Source on the Bottom Wall and Partially Cooled from Sides, *Thermal Science*, 18 (2014), Suppl. 2, pp. S283-S300
- [26] Cho, C.-C., et al., Enhancement of Natural-Convection Heat Transfer in a U-Shaped Cavity Filled with Al₂O₃-Water Nanofluid, *Thermal Science*, 16 (2012), 5, pp. 1317-1323

- [27] Rehan, M. A., *et al.*, Experimental Performance Analysis of Low Concentration Ratio Solar Parabolic trough Collectors with Nanofluids in Winter Conditions, *Renewable Energy*, 118 (2018), Apr., pp. 742-751
- [28] Duffie, J. A., Beckman, W. A., *Solar Engineering of Thermal Processes*, John Wiley and Sons Inc., Hoboken, N. J., USA, 2013
- [29] Chaudhary, G. Q., *et al.*, Small-Sized Parabolic trough Collector System for Solar Dehumidification Application: Design, Development, and Potential Assessment, *International Journal of Photoenergy*, 2018 (2018), 4, ID5759034
- [30] Patel, D. S, Patel, D. K, Thermal Analysis of Compound Parabolic Concentrator, *International Journal of Mechanical and Production Engineering Research and Development*, 5 (2015), 6, pp. 117-126